# Potential and Whole-genome Sequence-based Mechanism of Elongated-prismatic Magnetite Magnetosome Formation in Acidithiobacillus Ferrooxidans BYM

**Dan Zhao**
Heilongjiang Bayi Agricultural University
**Jiani Yang**
Heilongjiang Bayi Agricultural University
**Guojing Zhang**
Heilongjiang Bayi Agricultural University
**Dong Lu**
Institute of Modern Physics Chinese Academy of Sciences
**Shuang Zhang**
Heilongjiang Bayi Agricultural University
**Weidong Wang**
Heilongjiang Bayi Agricultural University
**Lei Yan** ( hekouyanlei@gmail.com )
HLAU: Heilongjiang Bayi Agricultural University

**Research**

**Keywords:** Magnetosomes, Acidithiobacillus ferrooxidans, Whole-genome, Formation mechanism, Gene prediction

**Posted Date:** September 28th, 2021

**DOI:** https://doi.org/10.21203/rs.3.rs-919317/v1

# Abstract

A magnetosome-producing bacterium *Acidithiobacillus ferrooxidans* BYM (*At. ferrooxidans* BYM) was isolated and magnetically screened. The magnetosome yield from 0.5896 to 13.1291 mg/g was achieved under different aeration rates, ferrous sulfate, ammonium sulfate, and gluconic acid concentrations at 30 °C. TEM observed 6–9 magnetosomes in size of 20–80 nm irregularly dispersed in a cell. STEM-EDXS and HRTEM-FFT implied that the elongated-prismatic magnetite magnetosomes with {110} crystal faces grown along the [111] direction. Whole-genome sequencing and annotation of BYM showed that 3.2 Mb chromosome and 47.11 kb plasmid coexisted, and 322 genes associated with iron metabolism were discovered. Ten genes shared high similarity with magnetosome genes were predicted, providing sufficient evidence for the magnetosome-producing potential of BYM. Accordingly, we first proposed a hypothetic model of magnetosome formation including vesicle formation, iron uptake and mineralization, and magnetite crystal maturation in *At. ferrooxidans*. These indicated that *At. ferrooxidans* BYM would be used as a commercial magnetosome-producing microorganism.


# 1 Introduction

Magnetotactic bacteria (MTB) are a multi-phyletic group of gram-negative prokaryotes and widely distribute in the soil, lakes, oceans, and underwater sludge, even exist in extreme environments [1]. They exhibit various morphotypes (rods, cocci, spirilla, vibrios, and ovoid) and are classified into 13 bacterial phyla according to the GTDB (Genome taxonomy database) taxonomy and 7 phyla based on the NCBI taxonomy, including Proteobacteria, Omnitrophica, Nitrospirae, Planctomycetota, Latescibacteria, Fibrobacterota and Desulfobacterota etc.[2]. They are characterized by their ability to produce magnetosomes and swim along the geomagnetic field lines. Only about 70 strains of MTB have been isolated in pure culture since one of them was independently discovered by Salvatore Bellini and Richard Blakemore in 1963 and 1975, respectively, such as *Magnetospirillum magneticum* MGT-1, *M. magneticum* AMB-1, *M. gryphiswaldense* MSR-1, *Magnetospirillum* sp. MSM3, *Magnetococcus* sp. MC-1, *Desulfamplus magnetovallimortis* BW-1 and so on [3]. Bacterial magnetosome is composed of phospholipid bilayer membrane-enclosed crystals of magnetite ($Fe_3O_4$) or greigite ($Fe_3S_4$). The size of mature magnetite crystals ranging from 35–120 nm is in a stable single magnetic domain [4]. The formation of magnetosomes were strictly controlled by the genes and consisted of several processes, including magnetosome vesicle formation, iron transportation and accumulation, redox control of magnetic crystal biomineralization, magnetosome chain assembly and morphological regulation [3]. It has been reported that more than 40 genes involved in the biosynthesis of magnetosomes [5]. The complete genome sequencing of MTB strains was first achieved in a model microorganism *M. magneticum* AMB-1 and then the genomes of about 17 strains of MTB have also become available. Comparative genome analysis of both cultured and uncultured MTB revealed the presence of a well-conserved region called the magnetosome island (MAI) in the chromosome and confirmed its functional significance in magnetosome formation. It has been suggested that MAI harbored the magnetosome gene clusters, structured as operons including *mamAB*, *mamGFDC, mms6, mamXY* and *feoAB*, can be acquired and transmitted via horizontal gene transfer [5]. Due to the unique properties such as ferrimagnetism, nanoscale size, narrow size distribution, dispersal ability, membrane-bound structure, and good biocompatibility, the magnetosomes could be applied in biomedicine, biotechnology, material science and environmental protection [4]. Additionally, their application in geology, mineralogy, oceanography and astrobiology would be worth exploring further.

Therefore, the high-yield production of magnetosomes from microorganisms is critical for commercial application. Most studies have been conducted to enhance magnetosome yields by optimizing conditions for bacterial growth or/and magnetosome synthesis, genetic construction of magnetosome high-yielding mutants, and protein-mediated

biomimetic synthesis of magnetosome-like particles *in vitro* [6]. Unfortunately, it is challenging to find a suitable artificial environmental condition to cultivate wild and mutant MTB due to their fastidious lifestyle, creating a major hurdle to relocate magnetosome production from laboratory level to industrial or commercial scale [7]. In addition, the magnetosome-like nanoparticles synthesized by the physical, chemical and biomimetic method *in vitro* are often non-uniform, incompletely crystalline, compositionally nonhomogeneous and easy to aggregate because of the magnetic attraction [8]. Furthermore, these artificial synthetic techniques are costly and energy-intensive due to the involvement of expensive toxic or hazardous chemicals which can be harmful to humans and the environment [7]. Thus, it is necessary to introduce unfastidious magnetosome-producing microbes regretless of their magnetotaxis.

It has been discovered that several easy-to-cultivate non-magnetotactic iron-oxidizing bacteria including *At. ferrooxidans*, *Ferroplasma thermophilum* and *Leptospirillum ferriphilum* can produce magnetosomes [4]. Among them, *At. ferrooxidans* is a gram-negative, extremely acidophilic chemolithoautotrophic bacterium and has been recognized as an important member involved in biogeochemical iron cycling [9]. It wildly distributes in nature and obtains energy through the oxidation of ferrous iron and/or reduced inorganic sulfur. It has been demonstrated that the magnetosomes synthesized by *At. ferrooxidans* exhibit the above-mentioned excellent characteristics possessed by MTB magnetosomes [10]. It was speculated that the formation mechanism of magnetosomes in *At. ferrooxidans* might be different from that in MTB, since a chromosomal region similar to MAI was not found in the whole genome of *At. ferrooxidans*. Although more than 500 isolates and several genomes of *At. ferrooxidans* have been reported, the insight into the molecular mechanism of magnetosome formation by utilizing the complete genome sequence is not provided. Additionally, the synthetic ability of magnetosomes of *At. ferrooxidans* were preliminarily evaluated in the previous studies at the shake-flask scale by monitoring the indirect indexes including intracellular iron content and the cellular coefficient of magnetism ($C_{mag}$) [11]. However, the magnetosome-producing potential should be assayed at the bioreactor scale by measuring the direct parameters such as the weight and number of magnetosomes, which would help to have an in-depth understanding of the magnetosome production ability of *At. ferrooxidans* and its potential as a magnetosome-producing bacterial resource.

In the present study, *At. ferrooxidans* BYM was isolated and screened by a combination of liquid and semisolid-plate magnetophoresis, and was phylogenetically identified by the 16S rRNA gene. The magnetosome-producing potential of *At. ferrooxidans* BYM cultivated in a 5 L aerated bioreactor under various incubation conditions were appraised by a direct weighing method. The shape, crystal lattice parameter and element composition of the magnetosomes were observed by STEM-EDXS and HRTEM-FFT. Additionally, the genome of *At. ferrooxidans* BYM was wholly sequenced and annotated to generate a comprehensive description of the mechanism that how *At. ferrooxidans* synthesized magnetosomes.

## 2 Materials And Methods

# 2.1 Isolation and magnetic screening

Soil samples were obtained from Baiyin copper mine (N36°55'41.02", E104°08'5.25") of Gansu Province, China. Two gram of soil sample was inoculated in 40 mL modified 9K medium consisting of 2.4 g/L $(NH_4)_2SO_4$, 0.1 g/L KCl, 0.5 g/L $K_2HPO_4$, 0.5 g/L $MgSO_4 \cdot 7H_2O$ and 0.01 g/L Ca $(NO_3)_2$, 40 g/L $FeSO_4 \cdot 7H_2O$ at pH 2.0 [11]. The cultures were incubated aerobically in a shaking incubator at 120 rpm and 30°C until the color of the medium turned reddish-brown. The isolation was carried out on an agar 9K medium plate (1.0% agar) using a serial dilution method. Discrete colonies were obtained after 7–10 days and incubated in 9K liquid medium. This procedure was repeated three times to obtain a purified strain and magnetic screening was performed. Briefly, a small hard ferrite magnet (2 mT) was

immediately placed close to a wall of microcosms. After about 1–2 h of magnetic enrichment, the bacteria adjacent to the magnet were transferred to the wide mouth of Pasteur pipette to further magnetic separation by the “race track” method [12]. The tip-end pipette containing the accumulated cells was broken off after collection for 30–60 min. The collected cells were then inoculated on a semisolid agar plate and aerobically cultured at 30 $^{o}$C. The test group plate was placed on an artificial magnetic field created by a permanent magnet (8 cm · 6 cm · 1 cm, 18 mT), whereas the control group plates was placed on the geomagnetic field [13]. The bacteria adjacent to the magnet were inoculated into the 9K liquid medium, and the brownish-red culture was diluted and plated on the solid plate after incubation. The cycling of magnetic screening was performed 10 times (Fig. S1). The well-isolated colony was picked and inoculated into 9K liquid medium for cell collection and analysis. All reagents used in this work were analytical grade.

## 2.2 16S rDNA-based identification

Two-gram bacterial cells from the logarithmic phase were collected according to the previous report [14]. The genomic DNA was extracted from the collected cells according to the manufacturer’s instructions by a commercially available DNA extraction kit (Biomed Biotechnology, Beijing, China), and was detected by agarose gel electrophoresis (1.0 %). The identification was done by 16S rDNA amplification using the forward primer 27F (5'-AGAGTTTGATCCTGGCTAG-3') and the reverse primer 1492R (5'-TACGYTACCTTGTTACGACTT-3') purchased from Shanghai sangon Biotech. The amplification reaction was carried out in a total volume of 25 μL consisting of 1 μL DNA, 1 μL each of forward and reverse primer (10 μM), 12.5 μL 2×Taq PCR Master Mix (Biomed Biotechnology, Beijing, China) and 9.5 μL dd$H_2O$. PCR was performed on a 2720 Thermal Cycler Instrument (Applied Biosystems, Foster City, USA) using the following program: initial denaturation at 94℃ for 5 min, followed by 30 cycles of denaturation of 94°C for 30 s, annealing at 55°C for 45 s, extension at 72°C for 1 min and a final extension of 5 min at 72°C. The PCR products were checked by 1.0% agarose gel electrophoresis and purified by AxyGEN Nucleic Acid Purification Kit (Axygen scientific, Inc, USA). The gel-purified products were sequenced by Sangon Biotech (Shanghai) Co., Ltd. The 16S rDNA gene contiguous sequences were analyzed using the ChromasPro software version 2.6.5 (Technelysium Pty Ltd, Tewantin, Australia) and assembled by DNAMAN software version 6.0 (Lynnon Biosoft, Quebec, Canada). The nucleotide sequence of 16S rDNA was used to find maximum similarity to the bacterial strains in the NCBI database. The phylogenetic tree was drawn using the neighbor-joining method in MEGA 5.0 (Temple University, Philadelphia, PA, USA) with the reference sequences obtained from NCBI GenBank.

## 2.3 Batch magnetosome-producing potential assay

*At. ferrooxidans* BYM was cultivated in a 5 L aerated bioreactor (Fig. S2) to improve the production of bacterial biomass. The air filtered by 0.22 μm Millipore membrane was pumped into bioreactor through a central glass draught tube installed 5 cm above the bottom by a CT-202 air pump (SenSen Group Co., Ltd., Zhoushan, China). The ventilatory capacity was controlled by LZB-4WB gas flowmeter (Xiangjin Flowmeter Factory, Xinghua, China). The air inlet and outlet of bioreactor were installed with filters (0.22 μm×25 mm, Lab instrument Co., Ltd., Shanghai, China). The temperature was controlled using a DK-S24 thermostatic water bath (Senxin Experimental Instrument Co., Ltd., Shanghai, China). Batch fermentation were carried out in the bioreactor with 10% (v/v) inoculation under different ferrous sulfate concentration (15, 25, 30, and 40 g/L), ammonium sulfate concentration (0.24, 0.72, 1.2, and 1.8 g/L), gluconic acid concentration (5, 15, 30, and 50 mM), and ventilatory capacity (0.5, 0.8, 1.2, and 1.5 L/min). After 90% ferrous ions oxidation, the bacteria were thought to have reached the beginning of the stable growth phase [15]. The cells were then collected and the magnetosomes were extracted to evaluate the magnetosome-producing potential of *At. ferrooxidans* BYM.

## 2.4 Extraction of magnetosomes

The cultures of *At. ferrooxidans* BYM were filtered using a porous metal filter (Chuangwei Filtration Equipment Factory, Haining, China) with the filter membranes (0.22 μm×50 mm, Xinya Purification Device Factory, Shanghai, China) and then washed with pH 2.0 $H_2SO_4$. The bacterial cells were collected until the filtrate did not contain iron ions monitored by the potassium thiocyanate (KSCN) method. The magnetosomes were extracted according to the protocol described by Yan et al [10], with some modifications. Briefly, cell suspension cultures containing approximately 0.5 g (wet weight) of *At. ferrooxidans* BYM cells, DNase (50 μg/ml), RNase (100 μg/ml), $MgCl_2$ (5mM) and 1% (w/v) lysozyme in 20 ml of 10 mM Tris–HCl buffer (pH 7.4), was incubated at 37°C for 1 h. Then the intermittent ultrasonic treatment was performed for 45 min in an ice bath with 3 s ultrasound and intermittent 5 s by using an ultrasonic generator (Ningbo Xinzhi Biotechnology Co., Ltd. Ningbo, China) operating at 40 kHz and 382.5 W. The treated cell suspension was diluted 2 times by Tris-HCl and transferred into another flat-bottomed test tube which was placed on the S pole of the magnet (2 mT). After magnetic adsorption for 1 h, the supernatant was removed and the magnetosomes gathered at the bottom were repeatedly washed with 10 mM HEPES (pH 7.4) buffer at least ten times and stored in 4 $^{o}$C. The extracted magnetosomes at each time were accurately weighted used an electronic analytical balance (Shanghai Tianmei balance instrument Co., Ltd., Shanghai, China).

## 2.5 TEM, STEM and HRTEM characterization

The harvested *At. ferrooxidans* BYM cells were fixed by glutaraldehyde (2.5%, v/v) at 4°C overnight, post-fixed in 1% (w/v) osmium tetroxide for 1h, dehydrated through a graded ethanol series (70%, 80%, 90%, 100%), and embedded with a mixture of EPON 812 and acetone. Ultrathin sections were obtained using a Leica UC7 ultramicrotome (Co. Leica Microsystems GmbH, Germany), stained with both uranyl acetate and lead citrate. Conventional TEM observations were performed with a JEM-2100 TEM (JEOL, Tokyo, Japan) at an accelerating voltage of 120 kV. Crystal lengths (along the long axis) and widths (perpendicular to the long axis) were measured from TEM images. The concentrated magnetosome samples of *At. ferrooxidans* BYM were dispersed by ultrasound in ethanol. The analyte solutions were dropped onto duplex film and used for investigation. High-resolution TEM (HRTEM) and scanning TEM (STEM) observations in high-angle annular dark field (HAADF) mode were carried out on an FEI Tecnai G2 F20 microscope (FEI Ltd., Hillsboro, OR, USA) operating at 200 kV. Element analysis was carried out by energy-dispersive X-ray spectroscopy (EDXS). The fast Fourier transform (FFT) analysis of HRTEM images was performed to investigate the crystals' structural parameters using RADIUS software (EMSIS GmbH, Mendelstrasse, Muenster, Germany).

## 2.6 Whole-genome sequencing and proposal of magnetosome formation mechanism

The bacterial genomic DNA was extracted and detected as mentioned above. The qualified genomic DNA samples were subjected to whole-genome sequencing using Illumina MiSeq and PacBio in Personal Biotechnology Co. Ltd (Shanghai, China). The filtered reads were assembled into contigs by the A5-miseq version 20160825. and the Canu v 1.6 (Maryland Bioinformatics Labs, Park, MD, USA), and then corrected by Pilon v 1.22 (Free Software Foundation, Inc., Boston, MA, USA) to gain the final genome sequence. The coding sequences (CDS) in the genome were predicted by GeneMarkS v4.32 (http://exon.gatech.edu/GeneMark/). The tRNAs and rRNAs of the genome were predicted by the software programs tRNAscan-SE v1.3.1 (http://lowel ab.ucsc.edu/tRNAscan-SE) and Barrnap v1.2 (https://github.com/tseemann/barrnap), respectively.

The assembled genome was annotated by the Kyoto Encyclopedia of Genes and Genomes (KEGG) (https://www.kegg.jp/kegg/), the Gene Ontology (GO) (http://geneo ntolo gy.org/), and the Evolutionary Genealogy of Genes: Non-supervised Orthologous Groups (eggNOG) (http://eggnogdb.embl.de/#/app/emapper). The circular map

of the genome was generated using Cgview v1.7.11 (http://circo s.ca). The direct repeats (DRs) and Spacers (interval region) were detected by CRISPRs finder tool (http://crispr.i2bc.paris-saclay.fr/Server/). Gene island was predicted by Island Viewer 4 (http://www.pathogenomics.sfu.ca/islandviewer/). The FASTA formatted sequences of the magnetosome genes obtained from NCBI database were separately blasted against the genome sequence of *At. ferrooxidans* BYM. The sequences shared high similarity with the magnetosome genes in the genome of *At. ferrooxidans* BYM were selected applying a cut-off value of E□0.01 and functionally predicted based on the published information.

## 2.7 Analysis

The oxidation ratio of ferrous iron was the ratio of oxidized and initial ferrous ion content. The concentration of ferrous iron was tested by the potassium dichromate titration method according to the previous study [11]. The magnetosome-producing potential was evaluated based on the yields of magnetosomes (mg/g), which was expressed as the dry weight ratio of magnetosomes (mg) to bacterial cells (g). All experiments were conducted in triplicate and the results were expressed as mean ± standard deviation. The statistical analysis was performed with OriginPro 9.0 software (OriginLab, Northampton, USA) by one-way analysis of variance followed by Student's t-test for pairwise comparison. The difference with p□0.05 was considered statistically significant.

## 2.8 Nucleotide accession number

The accession numbers for the 16S rRNA gene sequence and the whole genome sequence of *At. ferrooxidans* BYM (plasmid) were deposited in the NCBI database with the accession number KY923140 and CP082238 (CP082239), respectively.

# 3 Results And Discussion

## 3.1 Isolation, magnetic screening and identification

The distinct and vivid color change from colorless to red-brown can be easily observed by naked eyes after inoculating the soil samples into 9K medium in a shaking incubator with 120 rpm at 30°C for 2–3 weeks. The serially diluted cultures were separately spread on the surface of 9K solid medium and incubated at 30°C for 10 days. It can be observed that the bacterial colonies with an average diameter of 1.0 ± 0.2 mm appeared smooth, round or oval with the rust-colored raised center surrounded by a yellow zone (Fig. 1a), which was similar to the results reported by Yan et al. [14]. The single colony was scraped and inoculated into 9K liquid medium for incubation and magnetic enrichment. The Pasteur tube appeared a brown liquid after few minutes under the “race-track” liquid magnetic separation (Fig. 1c). It can be found that the bacterial cells from the tip end of a cut-off Pasteur tube showed weak magnetotaxis on the semisolid 9K plates under an artificial magnetic field, while the magnetostatic phenomenon did not occur in the case of no artificial magnetic field (Fig. 1d). After repeating these procedures, the bacterial cells were collected. SEM analysis showed that the morphology of the bacterium is rod-shaped with 0.2–0.4 μm in width and 0.8–1.4 μm in length (Fig. 1b), which was consistent with the previous report [16].

Sequencing results showed that the length of the 16S rDNA fragment of the isolate was 1429 bp. The NCBI BLAST sequence homology analysis showed the 16S rDNA of the isolate shared 99.93% similarity with *At. ferrooxidans* ATCC 19859, thus the isolate was named *At. ferrooxidans* BYM (Fig. 1e). It also can be found that the 16S rDNA of *At. ferrooxidans* BYM exhibited high similarity (> 97.0%) with six strains of *Acidithiobacillus* genus, whereas only showed 80.80% homology with *M. gryphiswaldense* MSR-1.

## 3.2 Magnetosome-producing potential assay

MTB usually mineralize membrane-bound intracellular iron crystals (magnetosomes) which enable the cells to align and swim along magnetic field lines in a preferred direction. The inorganic component of magnetosomes is magnetite ($Fe_3O_4$) or greigite ($Fe_3S_4$). In order to biomineralize magnetite, MTB require several orders of magnitude more iron than non-MTB, reaching up to 4.0% of their cell dry weight [17]. There are many similar characteristics between MTB and *At. ferrooxidans* such as morphological types, trophic type, motility, ecological distribution, and growth temperature. It has been reported that *At. ferrooxidans* can synthesize magnetosomes and contain more than 2.0% iron based on dry weight [11]. Thus, sufficient iron is the crucial substrate for magnetosome-producing bacteria to form magnetosomes. Results showed that *At. ferro*oxidans BYM can produce magnetosomes within a wide range of ferrous sulfate concentrations (15–40 g/L) (Fig. 2). It appeared that the cell dry weight of *At. ferrooxidans* BYM increased with the increase of ferrous sulfate concentration, but the yields of magnetosomes were found to increase first and then decrease. The maximum yields of 7.1137 mg/g magnetosomes occurred at 30 g/L ferrous sulfate. However, the magnetosome yields declined to 4.5294 mg/g when the ferrous sulfate concentration increased to 40 g/L. This finding was supported by the previous study in which the high concentration of ferrous iron promoted the growth of bacteria but inhibited the synthesis of magnetosomes [18]. Additionally, the previous works suggested that the intracellular iron content of *M. magneticum* AMB-1 cells presented a logarithmic increase with increasing external iron concentration from 10 to 100 μM. However, a mutant of *M. magneticum* AMB-1 lacking MAI which was unable to form magnetosomes can still incorporate a large amount of iron [19]. Therefore, the iron demand for the growth of MTB cell was not completely consistent with that for magnetosomes synthesis, which is similar to our result.

The genes associated with the synthesis of magnetosomes such as *mpsA*-like, *magA*-like and *mamB*-like existed in the chromosome of *At. ferrooxidans* BYM (Table 2). It has been reported that the highest expression level of these genes appeared at 150–200 mM of ferrous concentration, while the iron-deficient or iron-excessive conditions (Below or above 150–200 mM ferrous concentration) could adversely affect their expression [20]. Additionally, the jarosite precipitation formed by hydroxylation would increase with the increase of the ferrous concentration, which could gradually cover the bacterial surface and hinder the electron transfer from iron as well as proton diffusion from bacterial cells, resulting in the reduction of magnetosome formation [11].

Table 1
Comparison of the genome characteristics of *At. ferrooxidans* BYM and other *Acidithiobacillus* spp. available in GenBank database

| strains | Level | DNA types | Length (kb) | GC% | Predicted gene numbers | Protein |
|---|---|---|---|---|---|---|
| ATCC 53993 | complete | chromosome | 2885.04 | 58.90 | 2926 | 2779 |
| ATCC 23270 | complete | chromosome | 2982.40 | 58.80 | 3087 | 2909 |
| Hel18 | partial | chromosome | 3109.16 | 58.60 | 3179 | 2955 |
| BY0502 | partial | chromosome | 2976.67 | 56.80 | 3186 | 2821 |
| CCM 4253 | partial | chromosome | 3196.56 | 58.60 | 3278 | 3049 |
| IO-2C | partial | chromosome | 2716.89 | 58.70 | 2822 | 2620 |
| YQH-1 | partial | chromosome | 3111.22 | 58.60 | 3189 | 2956 |
| DLC-5 | partial | chromosome | 4184.22 | 57.60 | - | - |
| RVS1 | partial | chromosome | 2826.31 | 58.80 | 2888 | 2705 |
| YNTRS-40 | complete | chromosome | 3257.04 | 58.47 | 3339 | 3053 |
| | | plasmid | 47.104 | 56.43 | 70 | 46 |
| BY-3 | partial | chromosome | 3832.34 | 57.80 | 4067 | 3777 |
| BYM | complete | chromosome | 3208.389 | 58.54 | 3260 | 2184 |
| | | plasmid | 47.11 | 56.44 | 54 | 27 |

Table 2
Comparison of magnetosome numbers between *At. ferrooxidans* BYM to other magnetosome-producing bacteria.

| Strains | Nutritional type | Oxygen demand | Number per cell | Incubation time (h) | Refences |
|---|---|---|---|---|---|
| *M. magneticum* AMB-1 | chemoorganoheterotrophic | microaerophilic | 6–18 | 130 | [33] |
| *M. gryphiswaldense* MSR-1 | chemoorganoheterotrophic | aerobic and microaerobic | 26–43 | 60 | [37] |
| *M. magnetotacticum* MS-1 | chemoorganoheterotrophic | microaerophilic | 21.8 | 168 | [32] |
| *D. magneticus* RS-1 | chemoorganoheterotrophic | anaerobic | 40 | 168 | [34] |
| *Magnetospirillum* sp. ME-1 | chemoorganoheterotrophic | microaerophilic | 13–21 | 49 | [40] |
| *Magnetofaba australis* IT-1 | chemolithoautotrophic | microaerophilic | 2–10 | ≈168 | [12] |
| | chemoorganoheterotrophic | | 7–13 | ≈168 | [12] |
| *Gammaproteobacteria* SS-5 | chemoorganoheterotrophic | microaerophilic | 13–27 | ≈168 | [35] |
| *Gammaproteobacteria* BW-2 | chemoorganoheterotrophic | microaerophilic | 21–39 | ≈168 | [35] |
| *Candidatus Magnetobacterium bavaricum* LO-1 | Uncultured | microaerophilic | 100–200 | uncultured | [39] |
| *Rhodospirillum rubrum "magneticum"* | photoheterotrophic | anaerobic | 14 | 160 | [36] |
| *At. ferrooxidans* BY-3 | chemolithotrophic | aerobic | 3–5 | 48 | [11] |
| *At. ferrooxidans* 23270 | chemolithotrophic | aerobic | 2–4 | 146 | [38] |
| *At. ferrooxidans* BYM | chemolithotrophic | aerobic | 6–9 | 48 | This study |

One of the most important factors affecting microbial growth and magnetosome synthesis is oxygen. It has been demonstrated that magnetosome formation in MTB occurred only in a narrow range of low oxygen concentration. Dissolved oxygen (DO) was the major factor affecting the magnetosome production of *M. gryphiswaldense* MSR-1 and the yields in a microaerobic condition with 5–10 ppm oxygen was found to be 1.43 times higher than that in anaerobic condition [21]. The formation of magnetosomes in *M. magneticum* AMB-1 was favorably carried out at the low level of $O_2$ (≤ 18.7 μM), but was strongly inhibited under high $O_2$ concentrations (50–100 μM) [22]. The effect of oxygen on the magnetosome-producing potential of *At. ferrooxidans* BYM were investigated under different aeration rates (0.5–1.5 L/min). Results showed that the formation of magnetosomes produced at any given aeration rate and the yields of magnetosomes ranged from 0.5896 to 4.5336 mg/g (Fig. 2). It was observed that the bacterial biomass significantly increased with the increase of ventilatory capacity due to the typical aerobic characteristic of *At. ferrooxidans* BYM, while the magnetosome yields tended to saturation and decreased gradually with further increase of air supply. The low aeration rate might cause the low level of oxygen dissolved in 9K medium, which could inhibit the growth of *At. ferrooxidans* BYM, resulting in a lower final cell density and further a lower magnetosome

production. This finding indicated that the oxygen demand for cell growth of *At. ferrooxidans* BYM was higher than that for magnetosome formation.

It appeared that the magnetosome yields began to decrease once the aeration rate exceeded 1.2 L/min (Fig. 2). The enhancement of oxygen mass transfer in the fermentation system possibly caused by the increase of aeration rate could cause high autooxidation of ferrous ion [23], which would compete with biological oxidation mediated by bacteria, leading to an advice effect on the growth of *At. ferrooxidans* BYM. The reactive oxygen species (ROS) produced by the metabolism of *At. ferrooxidans* BYM with $O_2$ as the terminal electron acceptor can damage DNA ultimately leading to cell death. It has been reported that the formation of magnetosomes can efficiently scavenge the intracellular ROS in MTB [24]. Therefore, the magnetosome formation in *At. ferrooxidans* might play critical role in removing ROS to avoid damage to cells. These indicated that the suitable aeration rate can not only satisfy the oxygen requirement for bacterial oxidation of ferrous ions, but also maintain the balance between ROS scavenging and magnetosome formation.

Nitrogen source is also an important impact factor for the growth of MTB and magnetite magnetosome biomineralization. It can be seen from Fig. 2 that the ammonium sulfate in the concentration range of 0.24 to 1.80 g/L was well documented to favor magnetosome formation. The magnetosome yields increased from 2.0099 to 13.1291 mg/g with ammonium sulfate concentration (Fig. 2). It has been reported that there is a substantial demand for nitrogen to form proteins for the assembly of magnetosome vesicles [25]. Additionally, the magnetosome-associated membrane proteins play a significant role in magnetosome crystals growth inside MTB [26]. Therefore, in the case of a sufficient supply of nitrogen sources, *At. ferrooxidans* BYM can efficiently form magnetosomes. Generally, the formation of magnetosomes would be adversely affected once the concentration of ammonium sulfate exceeds a certain value. It can be observed that the magnetosome yields decreased to 7.6584 mg/g when the ammonium sulfate concentration exceeded 1.2 g/L. In such cases, the production of massive amounts of jarosite layer on the cell surface at high ammonia ion concentration could prevent the metabolism of bacteria [23], resulting in the reduction of magnetosome yield. Therefore, the nitrogen source was not only necessary for the cell growth of magnetosome-producing bacteria but was also essential for magnetosome formation. Our finding was consistent with the previous studies on MTB [21, 27]. It has been confirmed that $NaNO_3$ was more likely to favor the magnetosome formation of *M. gryphiswaldense* MSR-1 than $NH_4Cl$ and $(NH_4)_2SO_4$, since $NaNO_3$ was used as terminal electron acceptor to alternate oxygen for the survival of microaerobic MTB. Although the cell growth rate of *M. gryphiswaldense* MSR-1 increased by 27% with the increase of $NaNO_3$ concentrations from 20 to 60 mM, the magnetosome yields decreased [21]. Low nitrate concentration (0.004 M) was found to promote the magnetosome formation of *M. gryphiswaldense* MSR-1 significantly. In contrast, the magnetosome yield decreased but the cell growth was not affected in nitrate concentrations ranging from 0.01 to 0.02 M [27].

Although organic compounds usually appear adverse effects on the growth of *At. ferrooxidans*, our results suggested that the gluconic acid in concentrations ranging from 5 to 15 mM can promote the yields of magnetosomes from 2.6009 to 6.8854 mg/g (Fig. 2). The gluconic acid might act as an iron-chelating agent to chelate ferric ions and enhance the bioavailability of iron by forming ferric–ligand complexes. This phenomenon was in agreement with the results of Edouard Alphandéry et al., who noted the growth of *M. magneticum* AMB-1 and the production of magnetosomes were improved by the chelating agents including ethylenediaminetetraacetic acid (EDTA), ascorbic acid, citric acid, alendronic acid, and neridronic acid [28]. The magnetosome formation depended on siderophores with a high and specific affinity for the ferric ion to incorporate iron, which has been described in diverse groups of MTB [29]. It has been reported that *At. ferrooxidans* can synthesize several potential siderophore outer membrane receptors (OMRs) involved in transporting ferric ions to the cytoplasm [30]. Therefore, the ferric-chelating agents can

save energy consumption for synthesizing siderophores and OMRs, thus providing more energy for cell growth. Additionally, gluconic acid could alleviate the passivation formation and remove the precipitate layer on the surface of bacteria, since it can chelate with ferric iron of jarosite which is the main component for passivation and precipitate layer [28]. Thus, the adverse effect of ferrous iron metabolic by-products on nutrient mass transfer and energy metabolism of *At. ferrooxidans* BYM could be relieved to a certain extent, resulting in a favorable conidiation for bacterial growth and magnetosome formation. Moreover, the redox potential of the cultivation system of *At. ferrooxidans* is dominated by the ratio of dissolved ferric to ferrous ions. Adding gluconic acid might affect the redox potential and pH because jarosite formation can be eliminated or partially alleviated in high redox potential and low pH [31]. It was observed that the magnetosome yields began to decrease with the increase of the gluconic acid concentration ranged from 15 to 50 mM (Fig. 2). Two possible explanations for this phenomenon can be considered. One is that high concentration of organic chelating agent might cause toxicity to autotrophic *At. ferrooxidans* BYM and affect its growth. The other reason is that the reactive oxygen species generated as the result of the alcohol functional unbinding from iron could damage the out membrane of bacterial cells.

## 3.3 TEM, STEM and HRTEM observation

It has been documented that the magnetosomes exist as one, two, or multiple chains inside living MTB [3]. Due to the presence of these magnetosomes, MTB have the ability to move along the applied external magnetic field. It can be observed that *At. ferrooxidans* BYM was capable of synthesizing intracellular magnetosomes which were not arranged in chain but distributed irregularly in cells (Fig. 3a). The magnetotaxis and magnetism of *At. ferrooxidans* BYM are very weak (Fig. 1d), which might be attributed to the random distribution of magnetosomes, which is a way of storing iron sources in the cell [23].

TEM observation indicated that the number of magnetosomes per cell was 6–9 in *At. ferrooxidans* BYM (Fig. 3a, white arrows). A comparison of the magnetosome number between *At. ferrooxidans* BYM to other magnetosome-producing bacteria was shown in Table 2 [11, 12, 32–40]. Although the magnetosome number per cell of *At. ferrooxidans* BYM is similar to or lower than most MTB, *At. ferrooxidans* BYM is still promising for magnetosome production due to its mild culture condition, simple nutritional requirement, and short incubation time. The particle size of the magnetosomes in *At. ferrooxidans* BYM varied from 20 to 80 nm (Fig. 3a, b and i), which was similar to the finding in *At. ferrooxidans* BY-3 [15]. It has been addressed that the size of the mature magnetosomes in most MTB fall within a narrow range of 35–120 nm, which were in the magnetic-single- domain range [3]. Therefore, the magnetosomes formed in *At. ferrooxidans* BYM appeared a single-domain (SD) size, possibly resulting in the permanent magnetism of the magnetosomes and thus the weak magnetotaxis behavior of cells.

We performed STEM-EDXS elemental mapping and HRTEM investigations on the magnetosomes to localize and characterize the intracellular iron mineral phases. It appeared that *At. ferrooxidans* BYM accumulated iron and intracellularly formed amorphous granules with an elemental composition dominated by Fe, C, N and O (Fig. 5b-h). This indicated that the inorganic crystal was magnetite and composed of organic membrane. The finding was supported by the previous studies, in which the magnetosomes of MTB and ferrous oxidizers from freshwater were consisted of magnetite crystal and phospholipid bilayer membrane [4]. It can be seen from Fig. 5b (white arrows) and Fig. 5i that the crystals mainly exhibited elongated prismatic shape which usually existed in the MTB affiliated with the alpha, eta and gamma subclasses of Proteobacteria [5]. The presence of the irregular shaped crystals in Fig. 5b (black arrows) might be due to immaturity in magnetosome biomineralization. Additionally, no crystal defects such as twinning, stacking fault and cation vacancies were detected in the isolated magnetosomes (Fig. 5b and i), indicating that no obvious oxidization occurred within magnetite crystals during magnetosome extraction. The Fast Fourier Transform (FFT) analyses indicated that the magnetosome crystals expressed {110} crystal faces (Fig. 5j),

and the lattice spacing of nanoparticles was about 2.8 Å, which was consistent with the distance of the {111} crystal face. These results implied that the magnetite crystals elongated along the [111] direction. The similar finding was also reported in the previous studies. The lattice spacings of nanoparticles in *A. ferrooxidans* ATCC 23270 were found to vary from 2.43 to 2.95 in the previous study [38]. It has been reported that the magnetosomes in *M. magnetotacticum* MS-1 were elongated-prismatic and grew parallel to [111] direction [41].

## 3.4 Whole-genome sequencing and magnetosome-producing candidate gene prediction

The rapid development of genome sequencing has obtained the clear insight on the magnetosome-producing mechanism of MTB. Deciphering the whole genome sequence is necessary for understanding the genes involved in the formation process of magnetosomes. It has been reported that ten strains among more than 500 *At. ferrooxidans* sensu stricto isolates have been sequenced so far, but only three strains (ATCC 23270, ATCC 53993, YNTRS-40) were sequenced to obtain the complete genome sequences. Illumina sequencing showed that the genome of *At. ferrooxidans* BYM consisted of a circular chromosome of about 3208.389 kb with 58.54% GC content, ORF number of 3260, 3 CRISPRs, and a plasmid of 47.11 kb with a GC content of 56.44%, ORF number of 54. The genes categorized in “biological process”, “cellular component” and “molecular function” were determined in the genome of *At. ferrooxidans* BYM. The presence of numerous signal transduction components suggested that the *At. ferrooxidans* could greatly regulate the cellular function to adapt to varying environmental conditions. GO functional annotation indicated that a total of 314 genes and 8 genes closely were related to iron metabolism on chromosome and plasmid, respectively (Fig. 4). Among them, 94 genes were associated with iron-sulfur cluster binding, followed by 49 genes related to iron ion binding. The genes concerned with ferric iron transport, ferrous iron transport, iron assimilation and iron chelate transport participated in the multiple metabolic pathways of *At. ferrooxidans* BYM.

Blast analysis indicated that several genes possibly related to magnetosome formation existed in the genome of *At. ferrooxidans* BYM, including the major category *mam* genes, followed by *feoAB, magA*, *mpsA* and *mms6* (Table 3) [35, 42–47]. The result indicated that the *mamA*-like gene might exist in *At. ferrooxidans* BYM because the gene fragment in the genome of BYM shared 87.88% sequence identity with *mamA* from *Alphaproteobacterium* LM-1. It has been proved that the magnetosome-associated protein MamA encoded by *mamA* gene (651bp) covers the outside of magnetosomes and plays a critical role in protein sorting through protein-protein interactions [48, 49]. The function was found to be based on its special structure because MamA folds as a sequential tetratricopeptide repeat (TPR) protein with three protein–protein interaction sites including a concave site, a convex site, and a putative TPR repeat in *M. magneticum* AMB-1 and *M. gryphiswaldense* MSR-1. MamA self-assembles through its putative TPR motif and its concave site create a large homooligomeric scaffold that can interact with other magnetosome-associated proteins via the convex site [49]. It has been demonstrated that the TPR motifs existed in a wide variety of proteins from prokaryotes are important for cells to execute the desired functions such as protein transport, protein folding, transcription and splicing, and cell cycle control [48]. Additionally, another function based on studies of a *mamA* deletion mutant has been proposed that MamA appears to activate or prime the preformed magnetosomes to biomineralization. Deletion of *mamA* has no effect on magnetosome membrane invagination, but fewer crystals were formed in *M. magneticum* AMB-1 [50].

Table 3
A list of predicted genes related to magnetosome formation in *At. ferrooxidans* BYM.

| Predicted genes | Referenced genes | Locus | Source | Similarity (%) | E-value | Predicted function | References |
|---|---|---|---|---|---|---|---|
| *mamA*-like | *mamA* | JN406508 | *Alpha proteobacterium* LM-1 | 87.88 | 0.003 | activate the magnetosome vesicles, stabilize the magnetosome chain | [44] |
| *mamB*-like | *mamB* | KF787127 | *Magnetospirillum moscoviense* BB-1 | 83.78 | 0.001 | iron transport, magnetosome vesicle formation | [45] |
| *mamE*-like | *mamE* | JX628767 | *Gamma proteobacterium* SS-5 | 70.19 | 2e-05 | redox control, protein sorting | [35] |
| *mamM*-like | *mamM* | JX628771 | *Gamma proteobacterium* SS-5 | 87.88 | 0.005 | iron transport, magnetite nucleation and crystal growth | [35] |
| *mamO*-like | *mamO* | KF787139 | *Magnetospirillum marisnigri* SP-1 | 92.59 | 0.003 | magnetite nucleation, activation of MamE | [45] |
| *mamQ*-like | *mamQ* | JF429807 | *Alpha proteobacterium* SS-4 | 80.39 | 0.001 | membrane formation | [44] |
| *feoAB*-like | *feoAB* | EF120624 | *Magnetospirillum gryphiswaldense* MSR-1 | 68.41 | 2e-28 | iron transport | [43] |
| *magA*-like | *magA* | AB001699 | *Magnetospirillum magnetotacticum* MS-1 | 79.55 | 0.007 | iron uptake, iron transport | [46] |
| *mpsA*-like | *mpsA* | D87827 | *Magnetospirillum magneticum* AMB-1 | 64.82 | 4e-12 | membrane formation | [42] |
| *mms6*-like | *mms6* | AB096081 | *Magnetospirillum magneticum* AMB-1 | 89.66 | 0.002 | morphological regulation | [47] |

The genes of *mamB* in *M. moscoviense* BB-1and *mamM* in *Gammaproteobacterium* SS-5 separately shared 83.78% and 87.88% similarity with the sequences in *At. ferrooxidans* BYM (Table 2). It has been reported that MamB and MamM are conserved and abundant integral membrane magnetosome-associated proteins with a molecular weight of 31.9 and 34.4 kDa, respectively [51]. They were thought to be involved in iron transport during magnetosome formation because of their high similarity to the members of the cation diffusion facilitator family (CDF), which generally transport metal cations such as ferrous ions from the cytoplasm into intracellular compartments or into the extracellular space using the proton motive force [52]. These might be the reason that could account for the increase of magnetosome yields of *At. ferrooxidans* BYM with increasing ferrous sulfate concentration. It has been confirmed

that MamB not only serves as iron transporter in magnetite biomineralization, but also acts as a landmark protein to initiating the formation of magnetosome vesicle in a transport independent process [53]. The previous studies suggested that the stable expression of MamB depended on the presence of MamM which could protect MamB from proteolytic degradation due to complex formation [52]. Additionally, the stabilization of MamB and MamM was found to directly involve in the regulation of magnetite crystal growth in magnetosome formation [54]. Therefore, the potential proteins coded by *mamB*-like and *mamM*-like genes in *At. ferrooxidans* BYM might execute iron transport and crystal size control.

It has been reported that *mamE* and *mamO* genes might play critical roles in the early stage of magnetite magnetosome formation in *M. magneticum* AMB-1. MamE, a HtrA protease consisted of 655 amino acids in *M. gryphiswaldense* MSR-1, which is responsible for the regulation of the Fe(II)/Fe(III) ratio to promote magnetite nucleation, and also appears to play an important role in protein sorting to the magnetosome membrane [51, 54, 55]. Deletion of *mamE* can cause the empty magnetosome vesicles and the mislocalization of several proteins within the cell [55]. It was found that *mamE* gene in *Gammaproteobacteria* SS-5 shared 70.19% identity with the gene fragment (*mamE*-like) in *At. ferrooxidans* BYM (Table 2). The previous study showed that *Gammaproteobacteria* SS-5 isolated from the southeastern shore of the Salton Sea could mineralize octahedral magnetite crystal chains [35]. Similar to MamE, MamO is a second HtrA/DegP family protease containing 632 amino acids [56]. Additionally, MamO contains a degenerate active site, rendering it incapable of exerting protease activity. It has been reported that MamO can promote magnetosome formation through two genetically distinct, noncatalytic activities including the activation of MamE-dependent proteolysis of biomineralization factors and direct binding to transition metal ions [57]. The GO results indicated that 49 genes related to iron ion binding existed in *At. ferrooxidans* BYM. The *mamO* in *Magnetospirillum marisnigri* SP-1 displayed a strong homology (92.59%) with the sequence in *At. ferrooxidans* BYM, suggesting that the potential *mamO*-like gene in *At. ferrooxidans* BYM might specifically promote magnetite nucleation. It has been proved that MamK and MamJ play key roles in the formation of magnetosome chain in MTB [51]. However, we did not find the genes with high similarity to *mamK* and *mamJ* in genome of *At. ferrooxidans* BYM, which was supported by the TEM observation that the magnetosomes appeared to arrange dispersively.

Table 2 showed that the *mamQ* gene in *Alphaproteobacterium* SS-4 shared 80.39% sequence identity with the possible gene in *At. ferrooxidans* BYM. It has been suggested that magnetosome membrane formation was genetically induced via the *mamQ* gene by acting as a hub for the early organization of magnetosome proteins prior to membrane invagination. The deletion of *mamQ* in *M. magneticum* AMB-1 cells resulted in the complete loss of magnetosome formation [56]. It has been reported that an integral membrane protein MamQ with 273 amino acids was found to be homologous to the LemA protein family which bears a potential resemblance to BAR domain proteins and involves bending membranes in eukaryotic cells [51, 58].

It can be found that the *magA*-like gene might exist in *At. ferrooxidans* BYM due to it shared high similarity (79.55%) with *magA* sequence in *M. magnetotacticum* MS-1. MagA consisted of 434 amino acids was found to have high homology with the cation efflux proteins including the potassium ion-translocating protein KefC in *Escherichia coli*, and the putative $Na^+/H^+$-antiporter NapA from *Enterococcus hirae*. It has been reported that MagA was an iron transporter in *E. coli* which was confirmed by direct iron uptake measurements in membrane vesicles [59]. More importantly, the gene fragment with high similarity with *magA* gene was also found to exist in *At. ferrooxidans* 23270 and its maximum expression level occurred at 150–200 mmol/L ferrous [20]. In the present study, the highest magnetosome yield was observed when the concentration of ferrous sulfate was 30 g/L (Fig. 2). These results indicated that the potential protein coded by *magA*-like gene in *At. ferrooxidans* BYM could participate in the iron transport during the process of magnetosome formation.

It has been reported that *mpsA* with a length of 954 bp plays a key role in the formation of magnetosome membrane invaginated from cytoplasmic membrane. The MpsA protein consisted of 317 amino acids has been identified from *M. magneticum* AMB-1 [42]. It is homologous to acyl-CoA carboxylase of *E. coli*, which was classified under the category of lipid metabolism, providing evidence that the invagination of the cytoplasmic membrane to form magnetosome membrane were mediated by acylation [60]. The *mpsA* gene in *M. magneticum* AMB-1 was found to share 64.82% identity with the sequence in *At. ferrooxidans* BYM. These indicated that *mpsA*-like gene might play a critical role in the process of magnetosome formation in *At. ferrooxidans* BYM, which served a similar function in MTB. The previous report suggested that the *mpsA* gene in *At. ferrooxidans* reached the highest expression level at 150–200 mmol/L of ferrous and its expression increased with the decrease of oxygen concentration [61]. These findings indicated that *mpsA*-like gene was significantly affected by ferrous concentration and oxygen concentration and tightly associated with the magnetosome formation in *At. ferrooxidans*.

Mms6, a small acidic protein consisted of 136 amino acids in *M. gryphiswaldense* MSR-1 strain, was predicted to control the size of the magnetite crystal [62]. It was also isolated from *M. magneticum* AMB-1 along with Mms5, Mms7 and Mms13. The Mms6 protein has a low complexity hydrophobic N-terminal region with a hydrophobic glycine-leucine sequence, and a hydrophilic C-terminal region rich in acidic amino acids (aspartic-glutamic) with iron-binding activity [63]. It has been reported that the *mms6* gene deletion mutant of *M. magneticum* AMB-1 was found to synthesize the smaller magnetite crystals with uncommon crystal faces, while the wild-type and complementation strains synthesized highly ordered cubo-octahedral crystals [62]. The sequence of *mms6* gene in *M. magneticum* AMB-1 shared 89.66% similarity with the *mms6*-like sequence in *At. ferrooxidans* BYM, indicating Mms6 protein might regulate crystal morphology during magnetite biomineralization in *At. ferrooxidans* BYM.

## 3.5 Hypothetical mechanism of magnetosome formation in *At. ferrooxidans*

So far, the understanding of magnetosome formation and iron biomineralization process in the magnetosome-producing bacteria mainly comes from two model MTB strains *M. gryphiswaldense* MSR-1 and *M. magneticum* AMB-1 [5]. It has been demonstrated that the synthesis of bacterial magnetite magnetosomes is not a simple transformation from ionic iron to nano-magnetite particles, but includes a series of processes such as invagination of the cytoplasmic membrane, formation of magnetosome vesicles, iron uptake and transport, formation of iron mineral precursors and crystal nucleus growth and maturation [64]. The magnetosome gene island (MAI), a set of about 40 genes located in five operons including *mamGFDC*, *mms6*, *mamAB*, *mamXYZ*, and *feoAB*, was proved to involve in the step-wise magnetosome genesis mentioned above.

Therefore, based on the prediction of the magnetosome-producing candidate genes in *At. ferrooxidans* BYM and the information of magnetosome formation mechanism in MTB, we proposed a possible mechanism for the formation of magnetosomes in *At. ferrooxidans*. The hypothetical model of magnetosome formation in *At. ferrooxidans* is present in Fig. 5. The formation of magnetosomes in *At. ferrooxidans* is hypothesized to comprise three independent and constitutionally coupled processes. (1) The protein encoded by *mamA-like* gene could initiate invagination of the cytoplasmic membrane to form magnetosome membrane once the ferric uptake regulator (Fur) is able to sense the external ferrous iron ions. (2) The Fe(II) then transport from the outer membrane into the periplasm via the iron transporter FeoAB and/or Mnth. Meanwhile, a portion of Fe(II) is oxidized by Cyc1 and/or CycA1 to Fe(III) [9]. Then MamB-like, MamM-like and MagA-like proteins transport Fe(II) and Fe(III) into the magnetosome vesicle to generate hydrated ferric oxide ($Fe_2O_3 \cdot nH_2O$), which triggers the growth of magnetosome vesicle involving the proteins of MamB-like, MamQ-like and MpsA-like. (3) The dehydration and redox of hydrated ferric oxide simultaneously occurred to form the magnetite precursor with the involvement of MamE-like, MamM-like, MamO-like and Mms6-like

[3]. A stoichiometric ratio of Fe(III)/Fe(II) = 2:1 and the low redox potential inside magnetosome vesicle were regarded as necessary for crystal formation. Thus, the occurrence of the crystal nucleation mediated by MamM-like and MamO-like might result in the maturation of magnetosome from magnetite precursor.

## 4 Conclusion

A magnetosome-producing bacterium was successfully isolated and identified as *At. ferrooxidans* BYM capable of forming magnetosomes at 30 $^{o}$C under a wide range of operating parameters such as ferrous sulfate (15–40 g/L), ammonium sulfate (0.24–1.8 g/L), gluconic acid (5–50 mM), and aeration rate (0.5–1.5 L/min). TEM showed the magnetosomes in the size of 20–80 mM distributed irregularly in cells. STEM-EDXS and HRTEM-FFT indicated that the elongated prismatic magnetite magnetosome crystal with {110} crystal faces elongated along the [111] direction. The genome of *At. ferrooxidans* BYM is consisted of the chromosome and the plasmid, harboring a total of 322 genes closely related to iron metabolism. Ten genes involved in magnetosome formation were predicted but were not acquired by multiple gene-transfer events during the bacterial evolution. A hypothetic mechanism of magnetosome formation in *At. ferrooxidans* comprising magnetosome vesicle formation, iron uptake and mineralization, and magnetite crystal maturation was proposed. These findings would lay the foundation for more profound theoretical research and commercial development of the magnetosomes of *At. ferrooxidans* BYM in the future.

## Declarations

# Ethics approval and consent to participate

Not applicable.

# Consent for publication

All authors consent.

# Availability of data and materials

Most of the datasets supporting the conclusions of this article are included within this article. The datasets used or analyzed during the current study are available on reasonable request.

# Competing interests

The authors declare that they have no competing interests.

# Funding

This work is supported by the Talent Training Program under Special Funds Supporting the Development of Local Universities from the Central Finance (HFBE[2019]465), National Natural Science Foundation of China (41471201), Longjiang Scholar Program of Heilongjiang Province (Q201815), Heilongjiang Bayi Agricultural University Support Program for San Heng San Zong (TDJH201809), Heilongjiang Provincial Natural Science Foundation of China (LH2020C079), and Technology Program of Land Reclamation General Bureau of Heilongjiang (HKKY190406).

# Authors' contributions

LY contributed to conceptualization and validation, investigation and funding acquisition; DZ performed writing-original draft preparation; DZ and JNY performed writing-reviewing and editing; WDW provided methodology; SZ and GJZ performed data curation and visualization; DL was involved in supervision; LY performed project administration. All authors read and agreed to publish the final manuscript.

# Acknowledgements

Not applicable.

## References

1. Lin W, Pan Y, Bazylinski DA. Diversity and ecology of and biomineralization by magnetotactic bacteria. Environ Microbiol Rep. 2017;9:345–56.
2. Lin W, Zhang W, Paterson GA, Zhu Q, Zhao X, Knight R, Bazylinski DA, Roberts AP, Pan Y. Expanding magnetic organelle biogenesis in the domain bacteria. Microbiome. 2020;8:1–13.
3. Yan L, Zhang S, Chen P, Liu H, Yin H, Li H. Magnetotactic bacteria, magnetosomes and their application. Microbiol Res. 2012;167:507–19.
4. Yan L, Da H, Zhang S, López VM, Wang W. Bacterial magnetosome and its potential application. Microbiol Res. 2017;203:19–28.
5. Dieudonné A, Pignol D, Prévéral S. Magnetosomes: biogenic iron nanoparticles produced by environmental bacteria. Appl Microbiol Biotechnol. 2019;103:3637–49.
6. Kashyap S, Woehl TJ, Liu X, Mallapragada SK, Prozorov T. Nucleation of iron oxide nanoparticles mediated by Mms6 protein in situ. Acs Nano. 2014;8:9097–106.
7. Basit A, Wang J, Guo F, Niu W, Jiang W. Improved methods for mass production of magnetosomes and applications: a review. Microb Cell Fact. 2020;19:1–11.
8. Prozorov T, Bazylinski DA, Mallapragada SK, Prozorov R. Novel magnetic nanomaterials inspired by magnetotactic bacteria: Topical review. Materials Science Engineering: R: Reports. 2013;74:133–72.
9. Zhang S, Yan L, Xing W, Chen P, Zhang Y, Wang W. Acidithiobacillus ferrooxidans and its potential application. Extremophiles. 2018;22:563–79.
10. Yan L, Yue X, Zhang S, Chen P, Xu Z, Li Y, Li H. Biocompatibility evaluation of magnetosomes formed by Acidithiobacillus ferrooxidans. Materials Science Engineering: C. 2012;32:1802–7.
11. Yan L, Zhang S, Liu H, Wang W, Chen P, Li H. Optimization of magnetosome production by Acidithiobacillus ferrooxidans using desirability function approach. Materials Science Engineering: C. 2016;59:731–9.
12. Morillo V, Abreu F, Araujo AC, Almeida LGPd, Prast AE, Farina M, Vasconcelos ATRd, Bazylinski DA, Lins U. Isolation, cultivation and genomic analysis of magnetosome biomineralization genes of a new genus of South-seeking magnetotactic cocci within the Alphaproteobacteria. Front Microbiol. 2014;5:72.
13. Liu X, Liu W, Yan Y, WU H. Isolation of Acidithiobacillus ferrooxidans by using solid-plate magnetophoresis. China Biotechnology; 2006.
14. Yan L, Hu H, Zhang S, Chen P, Wang W, Li H. Arsenic tolerance and bioleaching from realgar based on response surface methodology by Acidithiobacillus ferrooxidans isolated from Wudalianchi volcanic lake, northeast

China. Electron J Biotechnol. 2017;25:50–7.
15. Yan L, Zhang S, Chen P, Wang W, Wang Y, Li H. Magnetic properties of Acidithiobacillus ferrooxidans. Materials Science Engineering: C. 2013;33:4026–31.
16. Zhang Y, Zhang S, Zhao D, Ni Y, Wang W, Yan L. Complete genome sequence of Acidithiobacillus ferrooxidans YNTRS-40, a strain of the ferrous iron-and sulfur-oxidizing acidophile. Microorganisms. 2020;8:2.
17. Schüler D, Baeuerlein E. Iron-limited growth and kinetics of iron uptake in Magnetospirillum gryphiswaldense. Arch Microbiol. 1996;166:301–7.
18. Yang C, Takeyama H, Tanaka T, Matsunaga T. Effects of growth medium composition, iron sources and atmospheric oxygen concentrations on production of luciferase-bacterial magnetic particle complex by a recombinant Magnetospirillum magneticum AMB-1. Enzyme Microbial Technology. 2001;29:13–9.
19. Amor M, Tharaud M, Gélabert A, Komeili A. Single-cell determination of iron content in magnetotactic bacteria: implications for the iron biogeochemical cycle. Environ Microbiol. 2020;22:823–31.
20. Liu W, Wu H, Liu X, Liu X. Influence of different Fe sources and concentrations on formation of magnetosomes in Acidithiobacillus ferrooxidans. Transactions of Nonferrous Metals Society of China. 2008;18:1379–85.
21. Jajan LH, Hosseini SN, Ghorbani M, Mousavi SF, Ghareyazie B, Abolhassani M. Effects of environmental conditions on high yield magnetosome production by Magnetospirillum gryphiswaldense MSR-1. Iran Biomed J. 2019;23:209–19.
22. Popa R, Fang W, Nealson KH, Souza-Egipsy V, Berquó TS, Banerjee SK, Penn LR. Effect of oxidative stress on the growth of magnetic particles in Magnetospirillum magneticum. Int Microbiol. 2009;12:49–57.
23. Zhang S, Yan L, Li H, Liu H. Optimal conditions for growth and magnetosome formation of Acidithiobacillus ferrooxidans. African Journal of Microbiology Research. 2012;6:6142–51.
24. Guo FF, Yang W, Jiang W, Geng S, Peng T, Li JL. Magnetosomes eliminate intracellular reactive oxygen species in Magnetospirillum gryphiswaldense MSR-1. Environ Microbiol. 2012;14:1722–9.
25. Moisescu C, Ardelean I, Benning LG. The effect and role of environmental conditions on magnetosome synthesis. Front Microbiol. 2014;5:49.
26. Cornejo E, Subramanian P, Li Z, Jensen GJ, Komeili A. Dynamic remodeling of the magnetosome membrane is triggered by the initiation of biomineralization. MBio. 2016;7:e01898-01815.
27. Wang X, Li Y, Zhao J, Yao H, Chu S, Song Z, He Z, Zhang W. Magnetotactic bacteria: Characteristics and environmental applications. Frontiers of Environmental Science Engineering. 2020;14:1–14.
28. Alphandéry E, Amor M, Guyot F, Chebbi I. The effect of iron chelating agents on Magnetospirillum magneticum strain AMB-1: stimulated growth and magnetosome production and improved magnetosome heating properties. Appl Microbiol Biotechnol. 2012;96:663–70.
29. Calugay RJ, Miyashita H, Okamura Y, Matsunaga T. Siderophore production by the magnetic bacterium Magnetospirillum magneticum AMB-1. FEMS Microbiol Lett. 2003;218:371–5.
30. Quatrini R, Jedlicki E, Holmes DS. Genomic insights into the iron uptake mechanisms of the biomining microorganism Acidithiobacillus ferrooxidans. J Ind Microbiol Biotechnol. 2005;32:606–14.
31. Bevilaqua D, LahtiTommila H, Garcia O Jr, Puhakka JA, Tuovinen OH. Bacterial and chemical leaching of chalcopyrite concentrates as affected by the redox potential and ferric/ferrous iron ratio at 22 C. Int J Miner Process. 2014;132:1–7.
32. Ali I, Peng C, Khan ZM, Naz I. Yield cultivation of magnetotactic bacteria and magnetosomes: a review. J Basic Microbiol. 2017;57:643–52.

33. Li J, Ge X, Zhang X, Chen G, Pan Y. Recover vigorous cells of Magnetospirillum magneticum AMB-1 by capillary magnetic separation. Chin J Oceanol Limnol. 2010;28:826–31.
34. Arakaki A, Shibusawa M, Hosokawa M, Matsunaga T. Preparation of genomic DNA from a single species of uncultured magnetotactic bacterium by multiple displacement amplification. Appl Environ Microbiol. 2010;76:1480–5.
35. Lefevre CT, Viloria N, Schmidt ML, Posfai M, Frankel RB, Bazylinski DA. Novel magnetite-producing magnetotactic bacteria belonging to the Gammaproteobacteria. The ISME Journal. 2012;6:440–50.
36. Mickoleit F, Rosenfeldt S, ToroNahuelpan M, Schaffer M, Schenk AS, Plitzko JM, Schüler D. High-Yield production, characterization, and functionalization of recombinant magnetosomes in the synthetic bacterium Rhodospirillum rubrum “magneticum”. Advanced Biology 2021:2101017.
37. Lohße A, Borg S, Raschdorf O, Kolinko I, Tompa É, Pósfai M, Faivre D, Baumgartner J, Schüler D. Genetic dissection of the mamAB and mms6 operons reveals a gene set essential for magnetosome biogenesis in Magnetospirillum gryphiswaldense. J Bacteriol. 2014;196:2658–69.
38. Wu L, Yang B, Wang X, Wu B, He W, Gan M, Qiu G, Wang J. Effects of single and mixed energy sources on intracellular nanoparticles synthesized by Acidithiobacillus ferrooxidans. Minerals. 2019;9:163.
39. Lefèvre CT, Frankel RB, Abreu F, Lins U, Bazylinski DA. Culture-independent characterization of a novel, uncultivated magnetotactic member of the Nitrospirae phylum. Environ Microbiol. 2011;13:538–49.
40. Ke L, Chen Y, Liu P, Liu S, Wu D, Yuan Y, Wu Y, Gao M. Characteristics and optimised fermentation of a novel magnetotactic bacterium, Magnetospirillum sp. ME-1. FEMS Microbiol Lett. 2018;365:fny052.
41. Pósfai M, Lefèvre C, Trubitsyn D, Bazylinski DA, Frankel R. Phylogenetic significance of composition and crystal morphology of magnetosome minerals. Front Microbiol. 2013;4:344.
42. Matsunaga T, Tsujimura N, Okamura Y, Takeyama H. Cloning and characterization of a gene, mpsA, encoding a protein associated with intracellular magnetic particles from Magnetospirillum sp. strain AMB-1. Biochemical and Biophysical Research Communications 2000, 268:932–937.
43. Rong C, Huang Y, Zhang W, Jiang W, Li Y, Li J. Ferrous iron transport protein B gene (feoB1) plays an accessory role in magnetosome formation in Magnetospirillum gryphiswaldense strain MSR-1. Res Microbiol. 2008;159:530–6.
44. Lefèvre CT, Schmidt ML, Viloria N, Trubitsyn D, Schüler D, Bazylinski DA. Insight into the evolution of magnetotaxis in Magnetospirillum spp., based on mam gene phylogeny. Appl Environ Microbiol. 2012;78:7238–48.
45. Dziuba M, Koziaeva V, Grouzdev D, Burganskaya E, Baslerov R, Kolganova T, Chernyadyev A, Osipov G, Andrianova E, Gorlenko V. Magnetospirillum caucaseum sp. nov., Magnetospirillum marisnigri sp. nov. and Magnetospirillum moscoviense sp. nov., freshwater magnetotactic bacteria isolated from three distinct geographical locations in European Russia. Int J Syst Evol Microbiol. 2016;66:2069–77.
46. Matsunaga T, Sakaguchi T. Molecular mechanism of magnet formation in bacteria. J Biosci Bioeng. 2000;90:1–13.
47. Arakaki A, Webb J, Matsunaga T. A novel protein tightly bound to bacterial magnetic particles in Magnetospirillum magneticum strain AMB-1. J Biol Chem. 2003;278:8745–50.
48. Nguyen HV, Suzuki E, Oestreicher Z, Minamide H, Endoh H, Fukumori Y, Taoka A. A protein-protein interaction in magnetosomes: TPR protein MamA interacts with an Mms6 protein. Biochemistry Biophysics Reports. 2016;7:39–44.

49. Zeytuni N, Ozyamak E, BenHarush K, Davidov G, Levin M, Gat Y, Moyal T, Brik A, Komeili A, Zarivach R: Self-recognition mechanism of MamA, a magnetosome-associated TPR-containing protein, promotes complex assembly. Proceedings of the National Academy of Sciences 2011, 108:E480-E487.
50. Komeili A, Vali H, Beveridge TJ, Newman DK: Magnetosome vesicles are present before magnetite formation, and MamA is required for their activation. Proceedings of the National Academy of Sciences 2004, 101:3839–3844.
51. Nudelman H, Zarivach R. Structure prediction of magnetosome-associated proteins. Front Microbiol. 2014;5:9.
52. Uebe R, Junge K, Henn V, Poxleitner G, Katzmann E, Plitzko JM, Zarivach R, Kasama T, Wanner G, Pósfai M. The cation diffusion facilitator proteins MamB and MamM of Magnetospirillum gryphiswaldense have distinct and complex functions, and are involved in magnetite biomineralization and magnetosome membrane assembly. Mol Microbiol. 2011;82:818–35.
53. Uebe R, Keren-Khadmy N, Zeytuni N, Katzmann E, Navon Y, Davidov G, Bitton R, Plitzko JM, Schüler D, Zarivach R. The dual role of MamB in magnetosome membrane assembly and magnetite biomineralization. Mol Microbiol. 2018;107:542–57.
54. Siponen MI, Adryanczyk G, Ginet N, Arnoux P, Pignol D. Magnetochrome: ac-type cytochrome domain specific to magnetotatic bacteria. Vol. 40: Portland Press Ltd.; 2012. pp. 1319–23. 1319–1323.
55. Quinlan A, Murat D, Vali H, Komeili A. The HtrA/DegP family protease MamE is a bifunctional protein with roles in magnetosome protein localization and magnetite biomineralization. Mol Microbiol. 2011;80:1075–87.
56. Murat D, Quinlan A, Vali H, Komeili A: Comprehensive genetic dissection of the magnetosome gene island reveals the step-wise assembly of a prokaryotic organelle. Proceedings of the National Academy of Sciences 2010, 107:5593–5598.
57. Hershey DM, Ren X, Melnyk RA, Browne PJ, Ozyamak E, Jones SR, Chang MC, Hurley JH, Komeili A. MamO is a repurposed serine protease that promotes magnetite biomineralization through direct transition metal binding in magnetotactic bacteria. PLoS Biol. 2016;14:e1002402.
58. Greene SE, Komeili A. Biogenesis and subcellular organization of the magnetosome organelles of magnetotactic bacteria. Curr Opin Cell Biol. 2012;24:490–5.
59. Nakamura C, Burgess JG, Sode K, Matsunaga T. An iron-regulated gene, magA, encoding an iron transport protein of Magnetospirillum sp. strain AMB-1. J Biol Chem. 1995;270:28392–6.
60. Tanaka M, Okamura Y, Arakaki A, Tanaka T, Takeyama H, Matsunaga T. Origin of magnetosome membrane: proteomic analysis of magnetosome membrane and comparison with cytoplasmic membrane. Proteomics. 2006;6:5234–47.
61. LIU X, WU C, WU H, XIE J. Influence of oxygen on magnetosome formation in Acidithiobacillus ferrooxidans. Nonferrous Metals Science and Engineering; 2016.
62. Tanaka M, Mazuyama E, Arakaki A, Matsunaga T. MMS6 protein regulates crystal morphology during nano-sized magnetite biomineralization in vivo. J Biol Chem. 2011;286:6386–92.
63. Rawlings AE, Liravi P, Corbett S, Holehouse AS, Staniland SS. Investigating the ferric ion binding site of magnetite biomineralisation protein Mms6. PLoS One. 2020;15:e0228708.
64. Li J, Menguy N, Roberts AP, Gu L, Leroy E, Bourgon J, Yang Xa, Zhao X, Liu P, Changela HG. Bullet-shaped magnetite biomineralization within a magnetotactic Deltaproteobacterium: implications for magnetofossil identification. Journal of Geophysical Research: Biogeosciences 2020, 125:e2020JG005680.

# Figures

Figure 1

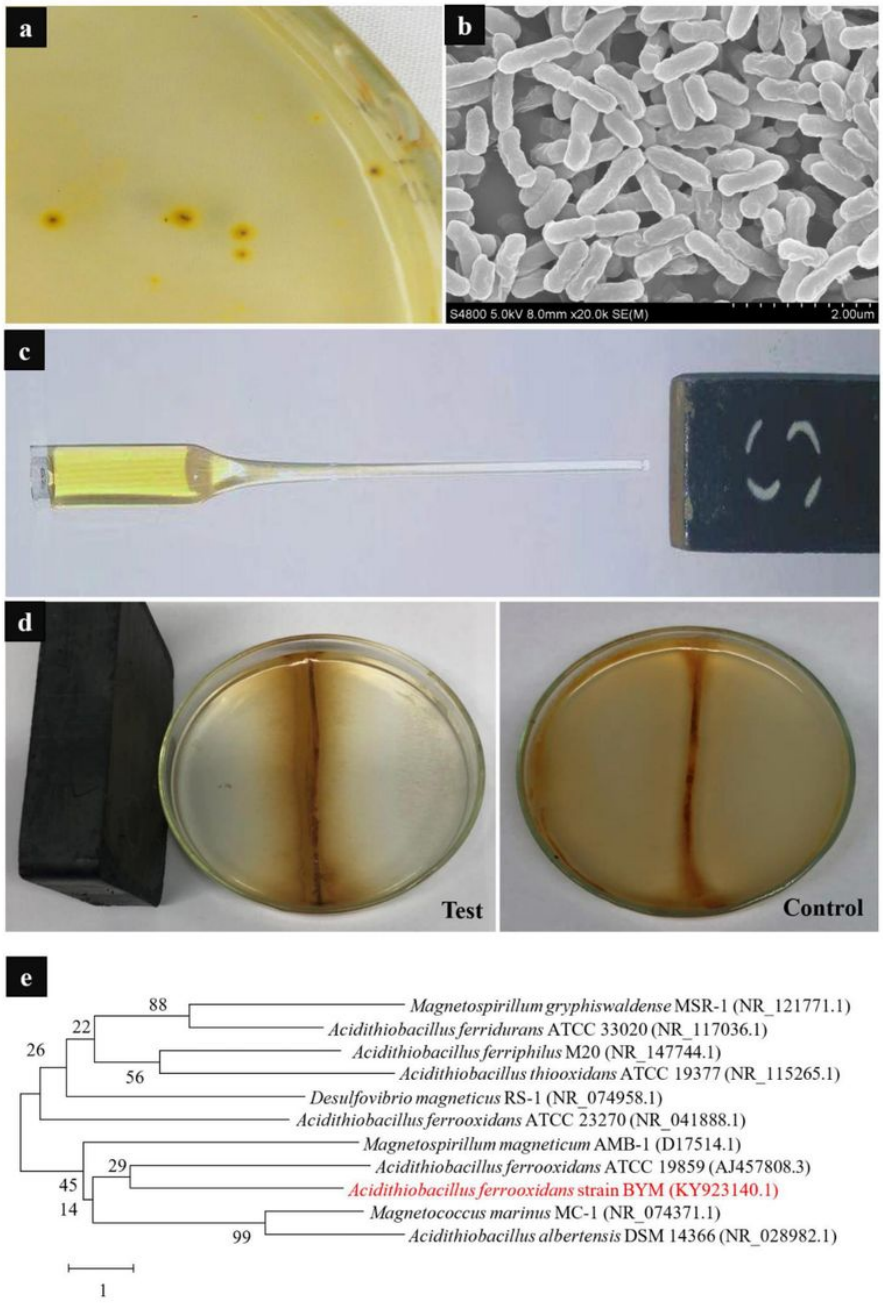


## Figure 1

Colony profile (a), cell morphology (b), race-track separation (c), magnetic swimming in semisolid agar plates (d) and 16S rDNA phylogeny (e) of BYM.

Figure 2

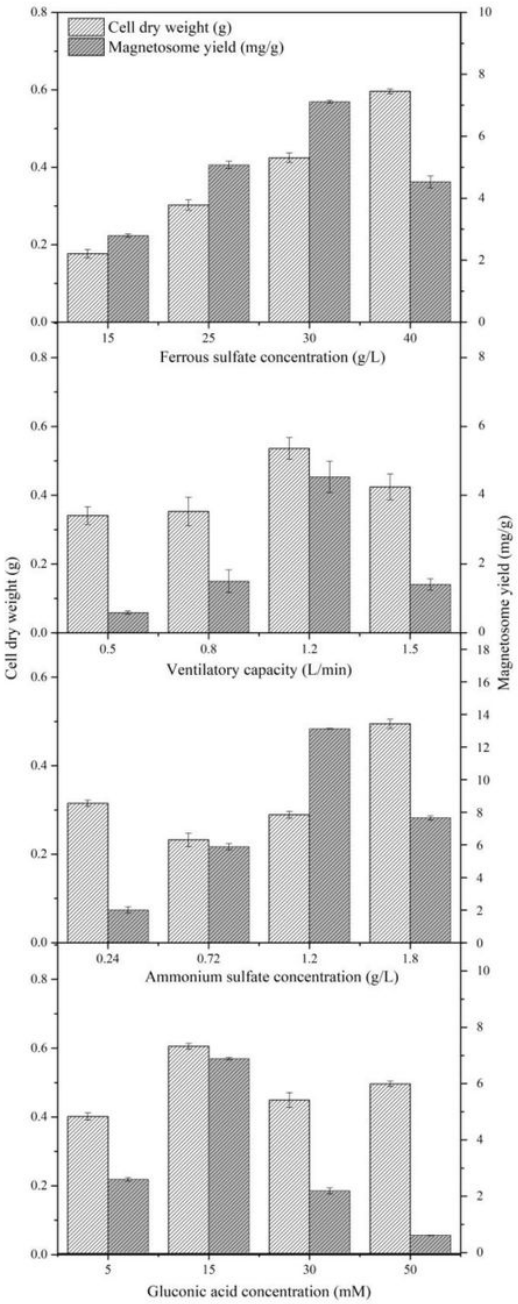


## Figure 2

Effects of ferrous sulfate concentration, ventilatory capacity, ammonium sulfate concentration and gluconic acid concentration on the magnetosome yield of At. ferrooxidans BYM.

Figure 3

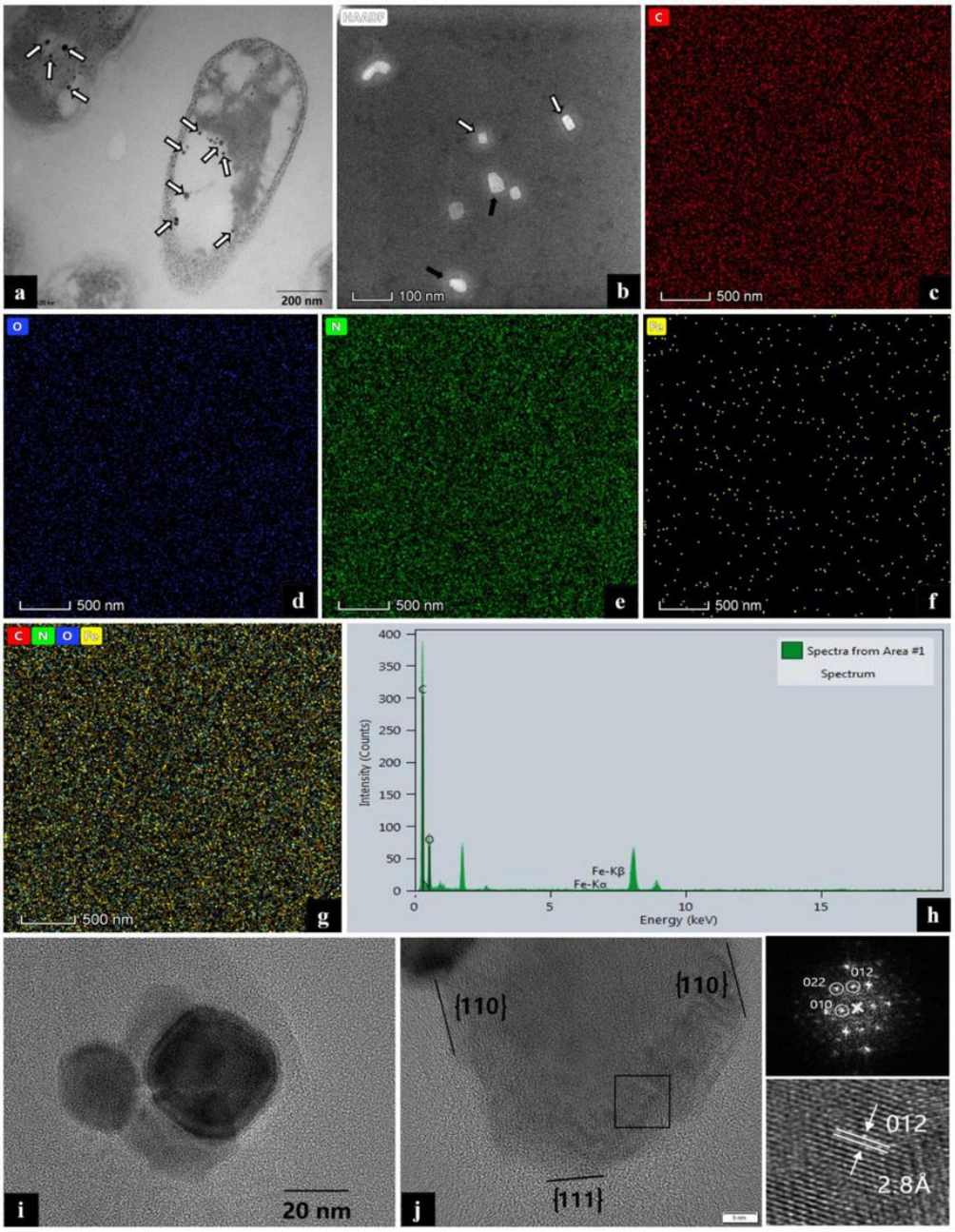


## Figure 3

TEM, STEM-EDXS and HRTEM observation. (a) TEM image of At. ferrooxidans BYM cells. (b-h) STEM-HAADF image of (b) extracted magnetosomes and corresponding elemental analysis of (c) C, (d) O, (e) N and (f) Fe; (g) RGB map with C (red), N (green), O (blue), and Fe (yellow); (h) EDXS spectra of extracted magnetosomes. (i-j) HRTEM images of (i) whole and (j) partial magnetosome crystal, the black square areas are corresponding indexed Fast Fourier Transform (FFT) patterns and image at higher magnification.

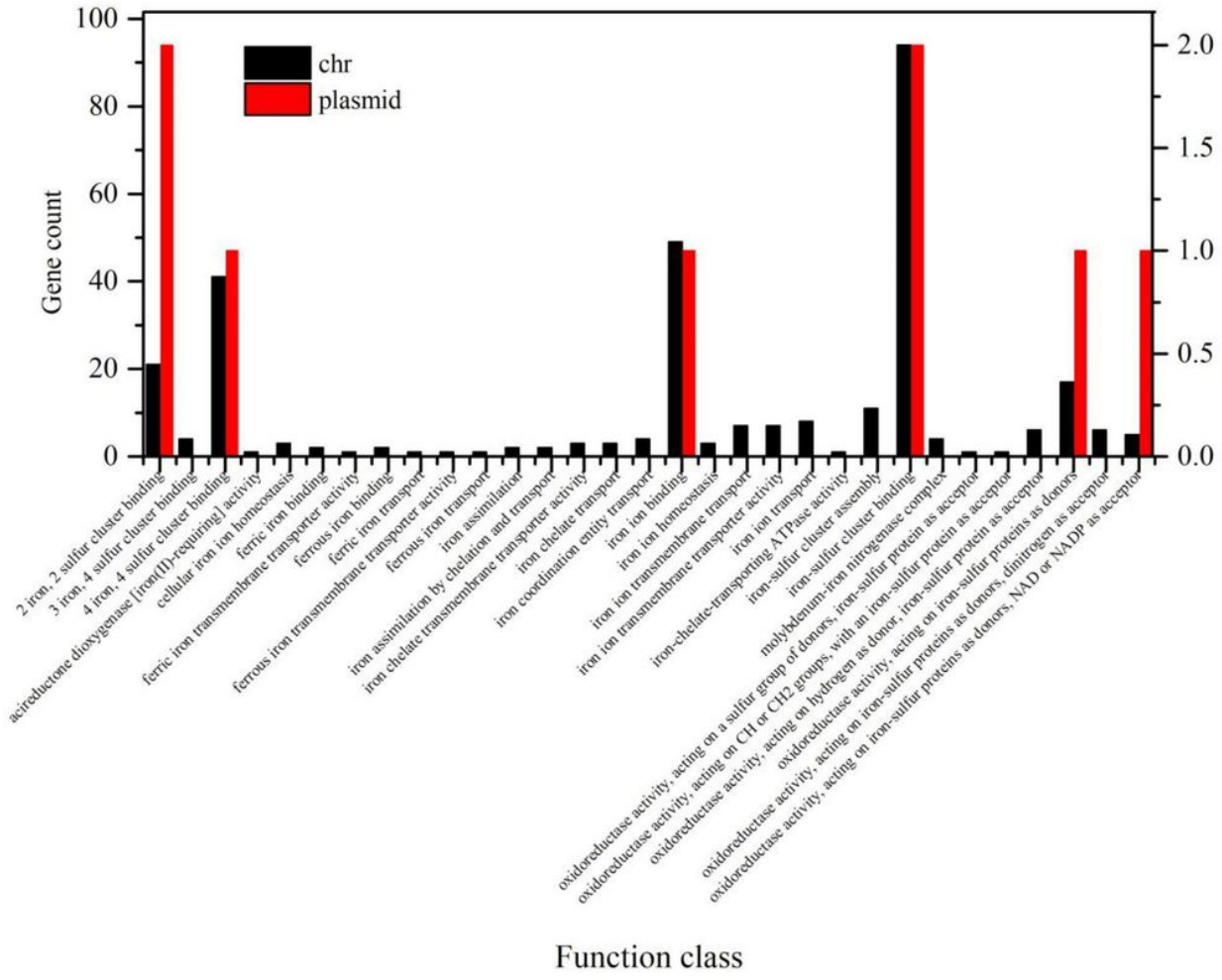


## Figure 4

Distribution of subsystem annotation related to iron metabolism on chromosome (black) and plasmid (red) of At. ferrooxidans BYM.

Figure 5

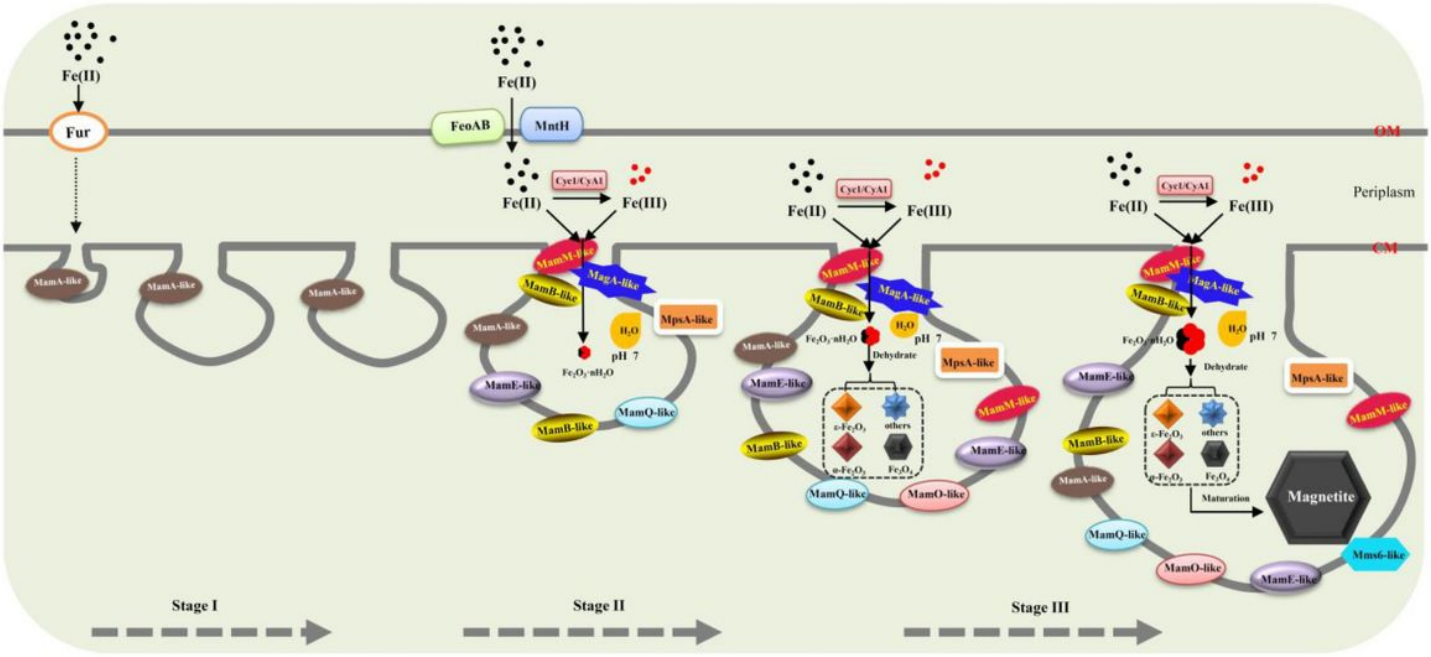


**Figure 5**

Hypothetical model for magnetosome formation in At. ferrooxidans BYM.

## Supplementary Files

This is a list of supplementary files associated with this preprint. Click to download.

- Graphicabstract.docx
- Supplementaryfigures.docx